Lidija PETKOVSKA[1,2], Goga CVETKOVSKI[2]

International Balkan University Macedonia (1), Ss. Cyril and Methodius University of Skopje (2)

Assessment of Torques for a Permanent Magnet Brushless DC Motor Using FEA

Abstract. This paper deals with magnetic field calculations and FE model-based prediction of torques in a PMBLDC motor. As a function of the rotor position, the torque produced by these machines has a pulsating component in addition to the dc component. This pulsating torque, according to the motor drive, has a fundamental frequency corresponding to six pulses per electrical revolution of the motor. The finite element analysis (FEA) has been employed to assess electromagnetic torque and cogging torque waveforms. The torque ripple in dependence of the switching angle for the control device is thoroughly investigated.

Streszczenie. Artykuł przedstawia obliczenia pola magnetycznego i predykcję momentu, bazujące na technice elementów skończonych, dla trójfazowych bezszczotkowych silnikach prądu stałego z magnesami trwałymi. Funkcją pozycji wirnika jest składnik pulsacyjny w momencie produkowanym przez te maszyny. Moment pulsacyjny, zgodnie z napędem silnika, posiada harmoniczną podstawową korespondującą od sześciu pulsów na jeden obrót wirnika. Metoda elementów skończonych została użyta do oszacowania momentu elektromagnetycznego oraz momentu żłobkowego. Zakłócenia momentu w zależności od kąta włączenia są szczegółowo badane. (Ocena momentów w bezszczotkowym silniku prądu stałego z magnesami trwałymi z wykorzystaniem metody elementów skończonych)

Keywords: Permanent brushless DC motor, Finite element analysis (FEA), Electromagnetic torque, Cogging torque, Torque ripple.
Słowa kluczowe: bezszczotkowy silnik prądu stałego z magnesami trwałymi, metod elementów skończonych, moment elektromagnetyczny, moment żłobkowy, zakłócenia momentu

Introduction

Nowadays, brushless direct current (BLDC) motors with permanent magnets (PM) are extensively used in a variety of drives. The demand for these high performance motors is continuously increasing in industrial applications because of their high efficiency and power density. Another advantage, over comparable motors, is the absence of the excitation winding. However, the PM motor inherently has a relatively high torque ripple which causes vibrations and noises. This deteriorates the performance of position control and speed control systems, particularly at lower speed [1]. Hence, it is important to find out accurate methods for calculation and assessment of the torques in Permanent Magnet Brushless DC (PMBLDC) motors, including the static electromagnetic toque and cogging torque, but in particular the torque pulsations, as well. In the paper analysis of torques, through numerical calculations of the magnetic field, is presented. It is started with computations of the static electromagnetic torque and cogging torque. The emphasis is put on determination and analysis of the torque pulsations, which appear due to the change of switching angles of the power supply and control device of the PMBLDC motor.

Topology of the PMBLDC Motor

The recent development of power semiconductors, high flux density rare-earth magnets, as well as advanced techniques for motor design and manufacturing, have led to increasing interest in applications of advanced permanent magnet brushless motors. The research has indicated that the PM motor drives, which include a brushless DC motor (PMBLDC) or a permanent magnet synchronous motor (PMSM), could become serious competitors to the induction motors for the industrial applications. The brushless DC motor has a trapezoidal back-emf and thus requires rectangular stator currents to produce constant torque, while the PMSM has a sinusoidal back-emf and requires sinusoidal stator currents to produce constant torque.

In the paper it is analysed one possible configuration of the PMBLDC motor drive: PM motor supplied and controlled by an AC-DC-AC power converter. The employed converter is either a current source of squared waves or a sine voltage source, which work is subordinated to the speed and the torque control through the stator current and rotor position regulation. The general scheme of the motor, its connection to the power supply, as well as all blocks necessary for the closed loop control system to work is presented in Fig. 1.
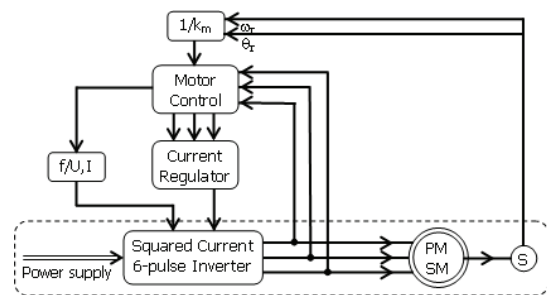

Fig.1. Topology of PMBLDC motor drive

The PM brushless DC motor that is studied in the paper is 3-phase, 6-pole, 36-slot machine, with rated current of 18 A, torque control 0-10 Nm, and speed control 0-4000 rpm. On the rotor surface of the motor, there are mounted six high energy S_mC_{o5} magnet poles that are magnetized in the radial direction, whilst the three-stage windings in a star (Y) connection are symmetrically placed in the stator slots [2].

Control Algorithm

The main functional blocks, surrounded by dashed line in Fig. 1 are: • the brushless DC permanent magnet motor, derived from a permanent magnet motor synchronous type (PMSM); • the rotor position sensor (S); • the three-phase full bridge six-pulse current inverter, which is presented in Fig. 2 more detailed. There are six transistors (T1–T6) that are placed in the upper and lower bank, connected in anti-parallel with a respective fly-back diode (D1–D6).
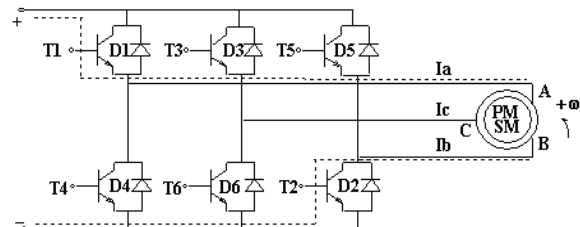

Fig.2. Transistor bridge inverter working in mode #1

Within one full electrical cycle (=$2\pi/p$ rad.mech.), six different switching modes in transistor gating sequence occur. At each moment, two transistors, one from each bank, are "*on*", thus supplying two of the stator windings with opposite current waves, while the third winding is left unexcited.
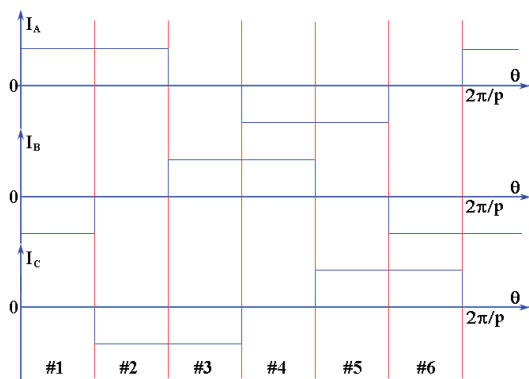
Fig.3. Current flow in the phase windings of the PMBLDC motor

When the commutation angle is neglected, the windings of PMBLDC motor are energised by alternate current waves with ideal rectangular profile, as presented in Fig. 3. Hence, the conduction of each phase winding is 40^0 mech., while every 20^0 mech. the current conduction mode is changed.

The control algorithm of PMBLDC motor and respective transistor switching modes (#1–#6) is arranged in Table 1.

Table 1. Control Algorithm of PMBLDC motor

Phase winding \\ Mode #	A	B	C	Triggered transistor
# 1 (A,B')	+I	–I	0	T1 & T2
# 2 (B',C)	+I	0	–I	T1 & T6
# 3 (A',C)	0	+I	–I	T5 & T6
# 4 (A',B)	–I	+I	0	T5 & T4
# 5 (B,C')	–I	0	+I	T3 & T4
# 6 (A,C')	0	–I	+I	T3 & T2

When only two phases of the motor are called upon to produce the same torque that three phases do, the current in each phase must be 3/2 as large, since:

$$(1) \qquad (3/2)\cdot(2 \text{ phases}) = (1)\cdot(3 \text{ phases})$$

As a result, if this drive scheme is implemented, the amplitude of the current waveforms shown in Fig. 3 must be modified to reflect this adjustment [3]. To summarise, the important aspects of the drive scheme include: • only six switches (transistors), which is a minimum number are required; • the phases do not produce torque in regions where their associated back emf is changing sign; thus, the back emf can be more trapezoidal than square; • each of the phases contributes an equal amount to the total torque produced; hence, each winding experiences equal losses and the drive electronics are identical for each phase.

Problem Definition

A drawback of permanent magnet brushless DC motors, which limits their wider applications, is the torque ripple characteristic caused by several reasons, between which the most important are: non-rectangular stator currents due to commutation from one phase to another, non-trapezoidal profile of the back-emf, and stator slot-tooth topology.

The cogging torque of the permanent motors is always a challenging matter for research and analysis. Cogging torque in DC brushless PM motors comes from variations in magnetic field density around the rotor permanent magnets as they pass the non-uniform geometry of the stator. The pulsating speed of the rotor, that cogging usually generates, may cause significant level of vibrations and noise. At high speed, this torque ripple is usually filtered out by the system inertia; however, at low speed, torque ripple becomes particularly undesirable and, in some special drive applications (e.g. servo drives), may not be tolerated [4].

The electromagnetic torque developed by the PM motor, and, consequently, the average and pulsating torques are mainly affected by the fluctuations of the magnetic field distribution, which in turn depends on the permanent magnet configuration, as well as the design of the slots and teeth. The accurate knowledge of the flux density profile that takes into account the direction of magnet bars magnetization along the magnet pole arc, the magnet topology (their width and height), the shape of stator slots and their number, the ratio of the rotor poles number versus the number of the stator teeth, as well as the air-gap length, are essential for accurate prediction of the PMBLDC motor performance.

Method of Analysis

Much research work has been performed to determine, to analyse, and to reduce torque ripple of the PM brushless DC motors. Some researchers have considered the torque ripple problem mainly from the design aspect [5], while the others have emphasized drive and control aspects [6]. The Finite Element Analysis (FEA), using either two-dimensional or three-dimensional field solver, has been used extensively in determination and evaluation of the electrical machines performance characteristics [7].

In this paper the authors link these two approaches, and develop a numerical tool for the torques assessment and analysis, based on the motor design parameters, but taking into consideration the control algorithm of the motor drive.

The results presented in this paper are computed using the 2D FEM code. As first step, the mesh of finite elements is generated over the whole radial cross section of the motor; it consists of more than 57,000 nodes and about 115,000 elements. In order to achieve a closer estimation of the torques, the mesh density has been particularly increased in the air gap, where the Maxwell stress is the highest. The combined PMBLDC motor geometry with the FE mesh and a zoomed-in part of the mesh are presented in Fig. 4.
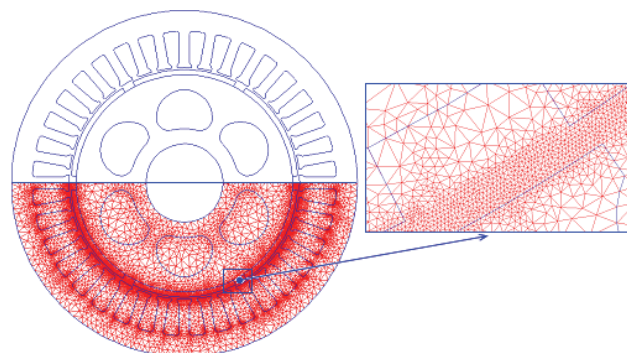

Fig.4. PMBLDC motor geometry and the FE mesh

The initial position 0^0 is arbitrary selected in accordance with Fig. 4, where the top PM-pole is with N-orientation; the displacement of the rotor is selected to be in the clockwise (CW) direction. The numerical calculations start with zero current in the stator windings, when the magnetic field is excited by the permanent magnets only; the numerical results of the torque are used for assessment the cogging torque of the PMBLDC motor.

The next computational FE results will show the effect of the load on the magnetic field distribution of the motor, and, in particular, on the electromagnetic torque. The numerical FE simulations of the magnetic field are performed including the control device work. For the mode #1, when the stator windings are energised with rated current 18A, as specified in the Table 1, i.e. for the current flow as depicted with dashed line in Fig. 2, the magnetic field distribution of the PM brushless DC motor is presented in Fig. 5 (a) to (e); the selected step for the rotor displacement is 5^0.
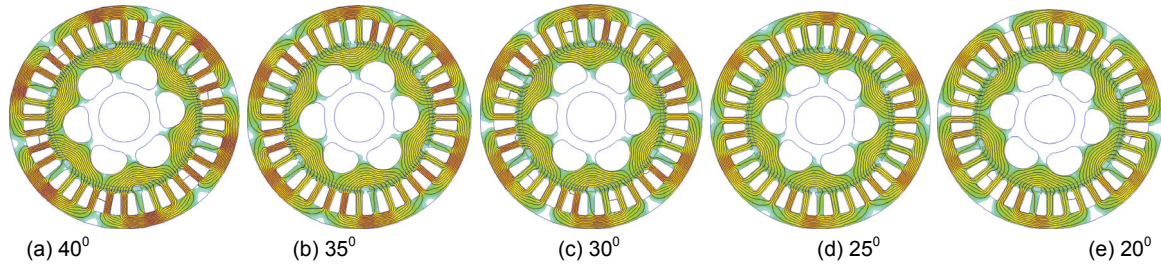
| (a) 40^0 | (b) 35^0 | (c) 30^0 | (d) 25^0 | (e) 20^0 |

Fig.5. Magnetic field distribution of the PMBLDC motor: current mode #1 and switching angle 40^0–20^0

FEM Computational Results

Assessment of the torques is very important matter for the performance analysis and a prediction of electric motor behaviour. The aim of the presented work is, by using FEA, to compute and analyse the static electromagnetic torque of the PMBLDC motor; introducing in the torque calculations zero current in the stator windings, the cogging torque profile is also derived and analysed. The particular emphasis is put on the calculations for both torque pulsations and torque ripple, when accounting the motor drive and control device. Accepting the conducting of 20^0 mech. at all modes #1–#6, the characteristics are derived in dependence of the switching –on and –off angles and are presented in figures; the numerical results are diagrammed and tabulated.

Electromagnetic torque

For the torque calculations, various approaches exist. The torque in an electric motor can be calculated either analytically or numerically in a variety of ways. Recently, many works have been published in this subject area. Although the attention is mostly put on analytical methods, the authors of the paper suggest the use of numerical finite element simulations. In general, they require very accurate global and local field solutions, particularly for determination of the cogging torque. In other words, a high level of mesh discretisation is required in a finite element calculation; the particular emphasis to this issue was put while developing the FE model of BLDCPM motor, as was explained before.

In the electromagnetic theory the torque is computed from the field solution in a number of ways. Recently, it has been shown that preferred method for calculating the electromagnetic torque is by weighted stress tensor of a volume integral in the air-gap. This approach greatly simplifies the computation of torques, as compared to assessing them via stress tensor line integral or by differentiation of co-energy, and is used in this paper; the results become more accurate with finer meshing around the region upon which the torque is to be computed, which has been shown in Fig. 4.

At mode #1, for the rated current 18A in the windings, the electromagnetic torque characteristic, spanned over one pole-pair pitch (120^0 mech.) is presented in Fig. 6.
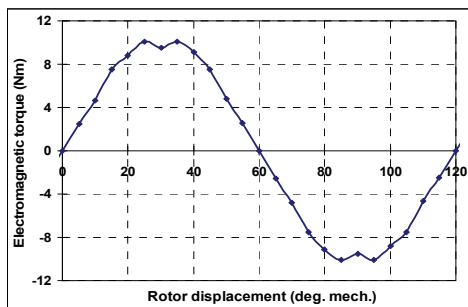

Fig.6. Electromagnetic torque characteristic T_{em}=f(θ) at $I=I_n$

The series of FE simulations for a variety of stator currents ($0–I_n$) and rotor displacements along a pole-pitch ($0–2\pi/2p$ rad.) are performed; thus, the full torque matrix T_{em}=f(I,θ) has been derived. The stator current is varied from I=0 to $I=I_n$=18A in steps of 3A, whilst the rotor is displaced along $0–60^0$ mech., in steps of 5^0.

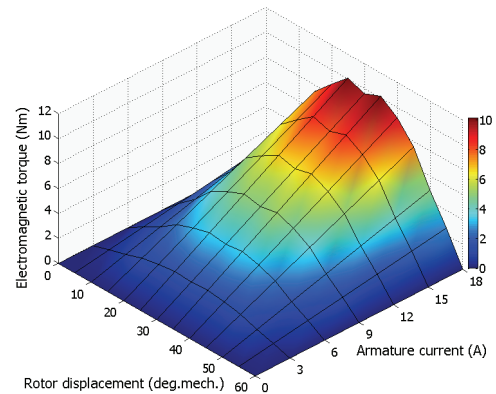The characteristics of the predicted electromagnetic torques are graphically presented and analysed.

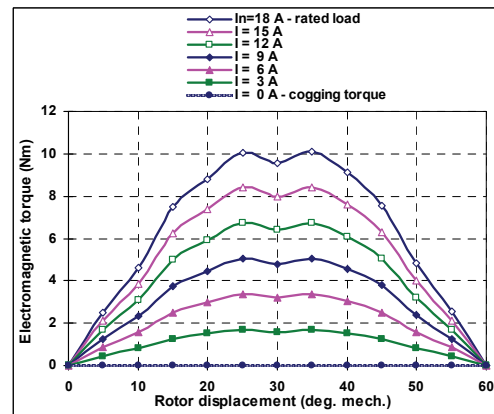Fig.7. Torque matrix T_{em}=f(I,θ) in 3D presentation

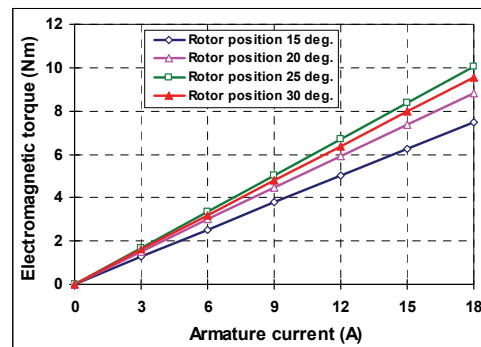Fig.8. T_{em}=f(θ), $I=cons.$ in Z–X plane

Fig.9. T_{em}=f(I),$\theta=cons.$ in Z–Y plane

The torque waveforms resulting from the simultaneous change of the stator currents and the rotor positions are given in the next diagrams, as follows: the 3D surface of the electromagnetic torque is shown in Fig. 7. The two other views in two planes Z-X and Z-Y, are presented in Fig. 8 and Fig. 9; they show two different sets of characteristics: T_{em}=f(θ), I=cons. and T_{em}=f(I), θ=cons., respectively. In Fig. 9 it is evident that there is a linear dependence between the static torque and the windings' current, which is in turn one of the main advantages of the controlled PM motor drives.

Cogging Torque

The cogging torque reduction of the PM motors has been always found as a problem to be solved. The pulsating speed of the rotor, that cogging usually generates, may cause significant levels of noise and vibrations. The cogging torque comes from the variations in magnetic field density around the rotor permanent magnets as they pass the non-uniform slot-tooth geometry of the stator; thus it is produced by the tendency of the rotor to align with the stator, at positions where the permeance of the magnetic circuit is maximized. Major factors affecting the cogging torque include PM magnetic field profile, air-gap length, stator slot openings, ratio of stator teeth and rotor poles numbers, and skewing. In addition, copper fill, pole pitch, flux distribution or density, magnet volume, and material weight can also influence both the peak value of the cogging torque and its profile. Relationships between some of these factors are difficult to be defined. Hence, the classical electromagnetic calculations do not provide either the data needed to determine accurately how much cogging torque might be developed in a motor, or the cogging profile.

A complete Finite Element Analysis (FEA) is an alternative method to be used. Although it usually consumes more computational time, it has been employed for this paper. Smooth and accurate prediction of the cogging torque requires not only a high number of mesh elements in the air-gap, but also very small angle of the rotor displacement inside the stator bore, causing a computational time to become excessive; otherwise, the torque profile calculated using FEA is not very smooth. The cogging (unexcited) torque of the PMBLDC motor, when the stator windings are not energised, is obtained from the FEM computational results. The characteristic T_{cog}=f(θ) along one period, i.e. the tooth pitch of 10^0, is presented in Fig. 10. The peak value is in the vicinity of 0.75 Nm, corresponding to approximately 7.5% of the rated electromagnetic torque.
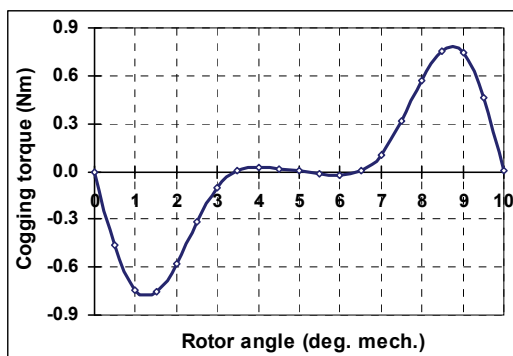

Fig.10. Cogging torque profile along a period

Torque ripple

Torque ripple is a critical concern in many applications of the PM motor drives, where low acoustic noise and high efficiency are strictly demanded. Consequently, the reduction of torque pulsations is an essential requirement in a wide range of high performance motion control applications, and they must be small enough.

There are mainly two contributions to the torque ripple in the PM motors. The first one is the cogging torque which arises, as was analysed and discussed before, from the interaction of the permanent magnets with the stator teeth. The second contribution is the torque pulsation due to the three main causes: (i) the first one is the non-sinusoidal shape of the currents in most brushless DC motors, resulting in presence of space harmonics in the air-gap flux density distribution; (ii) the second cause is the mismatch between the back-emf shape and the current shape; (iii) the third cause is the power converter control algorithm and operating cycle, resulting in time harmonics of higher order.

The particular interest in investigation of the PMBLDC motor performance is prediction and assessment of torque pulsations, due to the cause (iii). The fact that six times in a period (120^0 mech.), each with duration of $\Delta\theta$=20^0 mech., the transistor triggering is changed will result in 6 pulsations that are dependent on the time of the switching-on angle.

Introducing in the FE simulations the algorithm of the control device, different graphs are derived and analysed; the current in the stator windings is set to a rated value 18A, whilst the rotor is moving for $\Delta\theta$=20^0 in the CW direction.

The average value of the static torque, developed inside the interval $\Delta\theta$ for each triggering angle, is calculated from the following expression:

(1)
$$T_{av} = \frac{1}{\Delta\theta} \int_0^{\Delta\theta} T(\theta,I)d\theta \; |_{I=cons.}$$

For the basic case study is adopted to be the middle part of the electromagnetic torque profile, i.e. the interval 40^0 – 20^0. Due to the dip in the torque waveform that can be observed in Fig. 6, the pulsations profile will also have it. This dip is unwanted and must be reduced by optimising the motor cross-section topology.

The torque pulsations for a pair-pole pitch (120^0 mech.), are presented in Fig. 11 with shaded line. In the same figure, by a thin line is depicted expected ideal profile of the torque, whilst the average value of the toque determined from eq. (1) is drawn by the solid straight line.
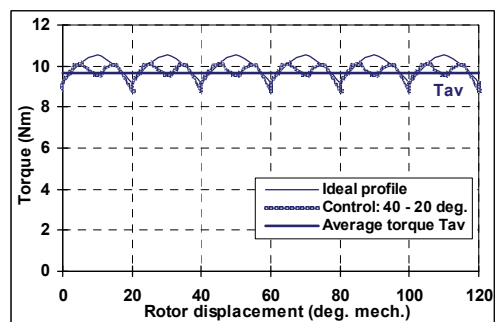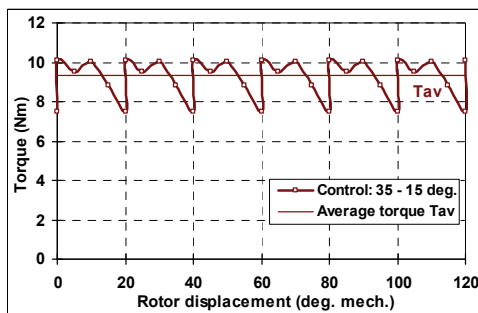

Fig.11. Torque pulsation: rated current and switching angle 40^0–20^0

In addition, for another three initial switching-on angles at mode #1, while keeping the rated current in the stator windings, the torque pulsation characteristics for PMBLDC motor are derived and presented in Fig. 12 (a), (b) and (c).

An important value, defining the stable operation of the permanent magnet brushless DC motor, is torque ripple R_T; it can be seen as a change of the peak torques (T_{max}, T_{min}) around the average torque value T_{av}; it is calculated from:

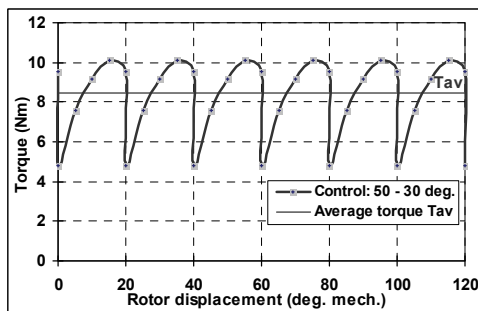$$(2) \qquad R_T = \frac{T_{max} - T_{min}}{T_{av}}$$

where: T_{max}, T_{min} – are peak values of the torque inside the interval $\Delta\theta$, while T_{av} is average torque for the studied case.

(a) rated current and switching angle $35^0 - 15^0$
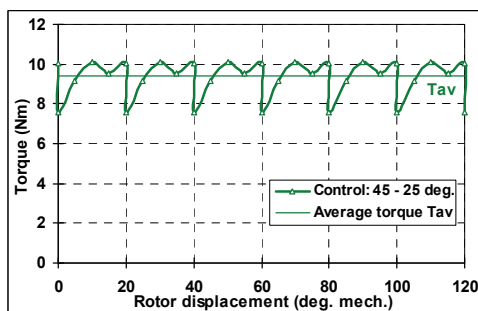
(b) rated current and $45^0 - 25^0$

(c) rated current and $50^0 - 30^0$

Fig.12. Torque pulsation characteristics for PMBLDC motor

The torque pulsation usually generates pulsating speed of the rotor, which causes vibrations and can significantly affect the performance of position control and speed control systems. The pulsation level of the torque is determined by the following equation:

$$(3) \qquad p_T = \frac{T_{max} - T_{min}}{T_{max} + T_{min}}$$

The values for T_{av}, R_T and p_T are calculated for selected conducting intervals, and are presented in Table 2.

Table 2. Torques for various switching of the current inverter

Switching $\theta_s \rightarrow \theta_c$ / Quantity	$35^o \rightarrow 15^o$	$40^o \rightarrow 20^o$	$45^o \rightarrow 25^o$	$50^o \rightarrow 30^o$
T_{max} (Nm)	10.103	10.103	10.103	10.103
T_{min} (Nm)	7.491	8.806	7.552	4.824
T_{av} (Nm)	9.303	9.670	9.398	8.494
R_T (p.u.)	0.281	0.134	0.271	0.621
p_T (p.u.)	0.148	0.069	0.144	0.354

Analysing the results from the table, the best triggering interval is found 40^0–20^0. Keeping the same value for the maximum torque developed by the motor, the value for the minimum torque is highest, leading to the highest average torque value. The PMBLDC motor will operate at minimum torque ripple of 13.4% and with pulsation level of only 6.9%.

Conclusion

FEA-based simulations have been performed to assess the waveforms of electromagnetic and cogging torque for the 0-10Nm&0-4000rpm PMBLDC motor. The finite element analysis (FEA) has been employed to study the motor performance, from the aspect of the torques. The stress is put on the analysis of the torque pulsation in dependence of the control device switching angle. The control algorithm 40^0–20^0 has been proved to be the best fitted, both to the maximum average torque and minimum torque ripple.

The next task is to optimise the motor topology in order to improve the electromagnetic torque profile, i.e. to avoid the dip, to minimise the torque pulsations caused by the cogging torque, as well as the torque ripple due to the motor drive operation. In the next calculations and analyses additional important factors will be included: magnetisation pattern of the permanent magnet bars, magnet skewing, as well as the shape of stator tooth tip. The results presented in this paper will serve as a good basis.

REFERENCES
[1] Gieras, J. F., Wing M. *Permanent Magnet Motor Techno-logy–Design and Applications*, pp. 227-310, New York, Basel: Marcel Dekker, Inc., 2002.
[2] Petkovska, L., Cundev, M. (1994) "Modelling and Dynamic Simulation of Permanent Magnet Motor", *Proceedings of 11th IEEE International Conference on Electrical Machines ICEM'94*, Vol. 3/3, pp.140-145, Paris, France
[3] Hanselman, D. C. *Brushless Permanent-Magnet Motor Design*, pp. 155-181, New York: McGraw-Hill, 1994.
[4] Ionel, D. M., Popescu, M., Mc Gilp, M. I., Miller, T. J. E., Dellinger, S. J. (2005) "Assessment of Torque Components in Brushless Permanent-Magnet Machines Through Numerical Analysis of the Electromagnetic Field", *IEEE Transactions on Industry Applications*, Vol. 41, No. 5, pp. 1149-1158.
[5] Jabbari, A., Shakeri, M., Niaki, A. N. (Winter-2010) "Torque ripple minimization in PM synchronous motors using tooth shape optimization", *Majlesi Journal of Mechanical Engineering*, Vol. 3, No .2, pp. 27-31.
[6] Shi, T., Guo, Y., Song, P., Xia, C. (2010) "A new approach for minimizing commutation torque ripple for brushless DC motor based on DC-DC converter", *IEEE Transactions on Industrial Electronics*, Vol. 57, 3483-3490.
[7] Petkovska, L., Cvetkovski, G., (2006) "FEM Based Simu-lation of Permanent Magnet Synchronous Motor Performance Characteristics", *Proceedings of CES/IEEE 5th International Power Electronics and Motion Control Conference IPEMC'06*, Vol. 1/3, pp. 254-258, Shanghai. China.

Authors: *Prof. Dr Lidija Petkovska, Ss. Cyril and Methodius University, Faculty of Electrical Engineering and IT, P. O. Box 574, 1000 Skopje, Macedonia, E-mail: lidijap@etf.ukim.edu.mk; Assoc. Prof. Dr Goga Cvetkovski, E-mail: gogacvet@etf.ukim.edu.mk;*